Diagn Interv Radiol 2024; DOI: 10.4274/dir.2024.242767

HEAD AND NECK IMAGING

ORIGINAL ARTICLE

Diagnostic performance of multishot echo-planar imaging (RESOLVE) and non-echo-planar imaging (HASTE) diffusion-weighted imaging in cholesteatoma with an emphasis on signal intensity ratio measurement

Ahmet Bozer[1]
Zehra Hilal Adıbelli[1]
Yeşim Yener[1]
Abdullah Dalgıç[2]

[1]İzmir City Hospital, Clinic of Radiology, İzmir, Türkiye

[2]İzmir City Hospital, Clinic of Otolaryngology Head and Neck Surgery, İzmir, Türkiye

PURPOSE

To evaluate the diagnostic efficacy of multishot echo-planar imaging (EPI) [RESOLVE (RS)] and non-EPI (HASTE) diffusion-weighted imaging (DWI) in detecting cholesteatoma (CHO), and to explore the role of signal intensity (SI) ratio measurements in addressing diagnostic challenges.

METHODS

We analyzed RS-EPI and non-EPI DWI images from 154 patients who had undergone microscopic middle ear surgery, with pathological confirmation of their diagnoses. Two radiologists, referred to as Reader A and Reader B, independently reviewed the images without prior knowledge of the outcomes. Their evaluation focused on lesion location, T1-weighted (T1W) signal characteristics, and contrast enhancement in temporal bone magnetic resonance imaging. Key parameters included lesion hyperintensity, size, SI, SI ratio, and susceptibility artifact scores across both imaging modalities.

RESULTS

Of the patients, 62.3% (96/154) were diagnosed with CHO, whereas 37.7% (58/154) were found to have non-CHO conditions. In RS-EPI DWI, Reader A achieved 89.6% sensitivity, 79.3% specificity, 87.8% positive predictive value (PPV), and 82.1% negative predictive value (NPV). Non-EPI DWI presented similar results with sensitivities of 89.6%, specificities of 86.2%, PPVs of 91.5%, and NPVs of 83.3%. Reader B's results for RS-EPI DWI were 82.3% sensitivity, 84.5% specificity, 89.8% PPV, and 74.2% NPV, whereas, for non-EPI DWI, they were 86.5% sensitivity, 89.7% specificity, 93.3% PPV, and 80% NPV. The interobserver agreement was excellent (RS-EPI, κ: 0.84; non-EPI, κ: 0.91). The SI ratio measurements were consistently higher in non-EPI DWI (Reader A: 2.51, Reader B: 2.46) for the CHO group compared with RS-EPI. The SI ratio cut-off (>1.98) effectively differentiated hyperintense lesions between CHO and non-CHO groups, demonstrating 82.9% sensitivity and 100% specificity, with an area under the curve of 0.901 (95% confidence interval: 0.815–0.956; $P < 0.001$). Susceptibility artifact scores averaged 1.18 ± 0.7 (Reader A) and 1.04 ± 0.41 (Reader B) in RS-EPI, with non-EPI DWI recording a mean score of 0.

CONCLUSION

Both RS-EPI and non-EPI DWI exhibited high diagnostic accuracy for CHO. While RS-EPI DWI cannot replace non-EPI DWI, their combined use improves sensitivity. SI ratio measurement in non-EPI DWI was particularly beneficial in complex diagnostic scenarios.

CLINICAL SIGNIFICANCE

This study refines CHO diagnostic protocols by showcasing the diagnostic capabilities of both RS-EPI and non-EPI DWI and highlighting the utility of SI measurements as a diagnostic tool. These findings may reduce false positives and aid in more accurate treatment planning, offering substantial insights for clinicians in managing CHO.

KEYWORDS

Cholesteatoma, diffusion-weighted imaging, non-EPI, RESOLVE, signal intensity ratio

Corresponding author: Ahmet Bozer

E-mail: drahmetbozer@gmail.com

Received 19 March 2024; revision requested 11 April 2024; last revision received 24 April 2024; accepted 08 May 2024.

Epub: 27.05.2024

Publication date: 06.11.2024

DOI: 10.4274/dir.2024.242767

You may cite this article as: Bozer A, Adıbelli ZH, Yener Y, Dalgıç A. Diagnostic performance of multishot echo-planar imaging (RESOLVE) and non-echo-planar imaging (HASTE) diffusion-weighted imaging in cholesteatoma with an emphasis on signal intensity ratio measurement. *Diagn Interv Radiol.* 2024;30(6):370-377.

Cholesteatoma (CHO), characterized by its invasive growth in the middle ear, poses substantial health risks, including hearing loss, vestibular disturbances, facial paralysis, and potential intracranial complications.[1] Accordingly, accurate diagnosis and effective treatment are essential. Magnetic resonance imaging (MRI) with diffusion-weighted imaging (DWI) serves as a critical tool for the initial assessment and diagnosis of CHO, as well as for monitoring local recurrence or residual CHO.[2] Due to its practicality and diagnostic efficacy, DWI has increasingly been adopted as a substitute for post-contrast sequences in MRI assessments.

The DWI techniques are primarily divided into two categories: echo-planar imaging (EPI)-based and non-EPI-based methods. Despite its rapid acquisition capability, single-shot (SS) EPI-DWI is susceptible to artifacts such as susceptibility, chemical shift, and geometric distortion.[3] These artifacts can obscure areas showing restricted diffusion, substantially compromising the detection of CHO. Additionally, the inherent limitations of EPI-DWI in terms of spatial resolution and section thickness pose challenges in detecting CHOs smaller than 5 mm.[4]

Recent technological advancements have led to the development of an improved multishot (MS) EPI technique that offers high-resolution DWI while reducing geometric distortions. However, this method necessitates longer imaging times. The RESOLVE DWI, utilizing a readout-segmented echo-planar [RESOLVE EPI (RS-EPI)] approach, introduces a cutting-edge method for capturing high-quality DWI images. This technique enhances image sharpness, increases spatial resolution, and reduces slice thickness,[5] thereby improving the detection of even small CHOs. By segmenting the k-space trajectory into multiple parts in the phase encoding direction, RESOLVE DWI reduces echo time (TE) and is substantially less affected by distortions, susceptibility, and T2* blurring artifacts, enhancing overall image quality.

Non-EPI DWI turbo spin-echo (TSE) is a spin-echo-based technique that can be applied in either SS or MS formats. It is renowned for its higher signal-to-noise ratio (SNR) and minimal image distortions, surpassing SS EPI-DWI in these respects. TSE provides enhanced spatial resolution in the middle ear, facilitating rapid multiplanar imaging and thinner slice capabilities compared with EPI sequences.[6] Moreover, TSE-DWI can be integrated with half-fourier acquisition SS TSE (HASTE), which offers excellent motion insensitivity and notably reduced susceptibility artifacts. Additional non-EPI DWI techniques, such as PROPELLER DWI and BLADE DWI, further minimize susceptibility artifacts and improve overall imaging quality.

The current body of literature features numerous studies that have compared standard EPI DWI with non-EPI DWI sequences in diagnosing CHO, consistently highlighting the superiority of non-EPI sequences.[7] Nevertheless, there have been limited studies comparing MS EPI sequences, such as RESOLVE, with non-EPI sequences. This study aims to assess the diagnostic performance of the MS EPI sequence, which offers shorter imaging times, as a viable alternative to non-EPI sequences. Furthermore, this research seeks to explore the role of signal intensity (SI) measurement in DWI, particularly when addressing diagnostic challenges, to potentially enhance the accuracy and reliability of CHO diagnosis.

Main points

- RESOLVE echo-planar imaging (RS-EPI) and non-EPI (HASTE) diffusion-weighted imaging (DWI) both demonstrate high diagnostic accuracy for cholesteatoma (CHO) individually. However, when used in conjunction, these techniques enhance diagnostic sensitivity.
- Signal intensity ratio measurements, particularly in non-EPI DWI, serve as a valuable quantitative tool for differentiating CHO from other conditions, thereby increasing diagnostic certainty.
- Susceptibility artifacts are minimal in RS-EPI DWI and completely absent in non-EPI DWI, underscoring the latter's potential for higher imaging quality and greater diagnostic value.

Methods

Patient selection and criteria

Following approval from the Clinical Research Ethics Committee of University of Health Sciences Türkiye, İzmir Bozyaka Training and Research Hospital (approval no: 2023/123, dated 23.08.2023), we conducted a retrospective single-center study. This study encompassed patients who underwent tympanoplasty and mastoidectomy for chronic otitis media (COM) between 2017 and 2023. Inclusion criteria included individuals with pre-operative temporal MRI scans featuring both RS-EPI and non-EPI (HASTE) sequences, as well as confirmed pathological diagnoses. The exclusion criteria were cases with incomplete or excessively artifact-laden MRI sequences and patients whose pathological results were inconclusive for diagnosis. Lesions located solely in the external acoustic canal (EAC) were also excluded. Ultimately, 154 patients met the criteria and were enrolled in the study.

Imaging technique

MRI was conducted using a 1.5T scanner (Siemens Healthineers, Magnetom Aera, Germany). Informed consent was obtained from all participants prior to imaging. The imaging protocol comprised axial T2-weighted (T2W) SPACE and T2W TSE sequences with fat saturation alongside axial and coronal T1-weighted (T1W) TSE sequences. Additionally, the protocol included coronal RESOLVE for DWI and apparent diffusion coefficient sequences, as well as coronal HASTE DWI. Post-contrast imaging was performed using axial and coronal T1W TSE sequences with gadobutrol (Gadovist™, Bayer AG, Berlin, Germany, 0.1 mmol/kg).

The RESOLVE DWI parameters were as follows: TR/TE: 3,780/60 ms; flip angle: 180°; 15 slices; slice thickness: 2.5 mm; *b* values (s/mm^2) = 0–1,000; field of view (FOV): 218; and matrix: 160 × 104, with an imaging duration of 2 minutes and 55 seconds. The HASTE DWI parameters included TR/TE: 2,000/103 ms; flip angle: 150°; 11 slices; slice thickness: 3 mm; *b* value (s/mm^2): 1,000; FOV: 220; matrix = 192 × 144; and an imaging time of 3 minutes and 42 seconds.

Imaging analysis

Two radiologists, with 32 years (Reader A) and 7 years (Reader B) of neuroradiological experience, respectively, independently assessed the MRI scans of the patients at workstations (Siemens Healthineers) without prior knowledge of the pathological outcomes. The study focused on patients who underwent surgical treatment and had a confirmed diagnosis, assessing both ears in each case.

The evaluation process commenced with an examination of standard temporal MR sequences. Lesion locations were categorized into several groups: middle ear; mastoid antrum; a combination of both; or middle ear and EAC.

The analysis proceeded with the selection of a single diffusion sequence for each patient, chosen randomly without a predetermined order. Approximately 1 month after completing the initial evaluations for all patients, the second diffusion sequence was reviewed. Lesions demonstrating hyperintensity in diffusion sequences relative to the

brain parenchyma were classified as diffusion-positive; those that did not were classified as diffusion-negative.[2,8]

For the radiological assessment, both the RS-EPI and non-EPI sequences were reviewed for each ear to determine the presence or absence of CHO. A positive finding in at least one of the sequences led to a radiological conclusion of CHO presence; absence in both indicated no CHO (Figures 1, 2).

The maximum diameter of hyperintensity was measured in the coronal plane for both diffusion sequences. Additionally, using a region of interest (ROI) approach, the SI of the area showing the highest hyperintensity and the SI of the temporal cortex on the same side were measured. The size of the ROI varied depending on the lesion size, and signal measurements were not performed in cases without diagnostic hyperintensity.

Susceptibility artifact scores were assigned as follows: 0 for no artifact; 1 for artifacts at the skull base; 2 for artifacts below the skull base; and 3 for artifacts interfering with diagnosis (Figures 1, 3). These scores were noted for both the RS-EPI and non-EPI DWI sequences and were included in the statistical analysis, considering the side (right or left) that underwent surgery.

Lesion T1W signal characteristics were categorized as either iso-hypointense or hyperintense relative to cerebral white matter. Post-contrast T1W enhancement of lesions was classified into four categories: no enhancement; peripheral enhancement; homogeneous enhancement; or heterogeneous enhancement.

Surgical and pathological confirmation

All patients included in the study underwent microscopic middle ear surgery, with histopathological results subsequently analyzed. For those diagnosed with CHO, the presence of the condition was confirmed both intraoperatively -indicated by the detection of keratinized squamous epithelium and debris within the middle ear- and through histopathological examination. Conversely, the non-CHO group comprised patients for whom no CHO was detected during surgery, a finding supported by histopathology, which confirmed the diagnosis of COM.

Statistical analysis

The data analysis was conducted using SPSS version 26 (IBM Corp., Armonk, NY, USA). Continuous variables were summarized using the mean, standard deviation (SD), and median interquartile range. Categorical variables were presented as frequencies and percentages. The distribution of continuous variables was assessed through graphical methods, normality tests, and consideration of sample size to determine normalcy.

Comparisons between independent groups were made using both the Student's t-test and the Mann–Whitney U test, depending on the distribution of the data. The Wilcoxon signed ranks test was employed for related samples. The distribution of categorical variables across independent groups was analyzed using the chi-square test. Changes in related samples were assessed using the McNemar test and the McNemar–Bowker test.

The agreement between the observations of the two radiologists and the pathological results was quantified using kappa (κ) values. Diagnostic test values, such as sensitivity, specificity, positive predictive value, and negative predictive value, were calculated based on the radiologists' assessments and compared with the pathology results. For all statistical tests, the significance level for type I error was set at α: 0.05, and the tests were conducted as 2-tailed.

Results

In this study, we evaluated 154 patients, comprising 94 men and 60 women, with a mean age of 44.79 years (± SD of 16.78 years). Of these, 96 patients (62.3%) were allocated to the CHO group, whereas 58 patients (37.7%) were classified in the non-CHO group.

Reader A identified CHO in 86 out of 96 patients (89.5%) in the CHO group using both RS-EPI and non-EPI DWI sequences. Reader B detected CHO in 79 out of 96 patients (82.3%) with RS-EPI DWI and in 83 out of 96 patients (86.5%) with non-EPI DWI within the same group. In the non-CHO group, Reader A correctly identified 46 out of 58 patients (79.3%) as not having CHO using

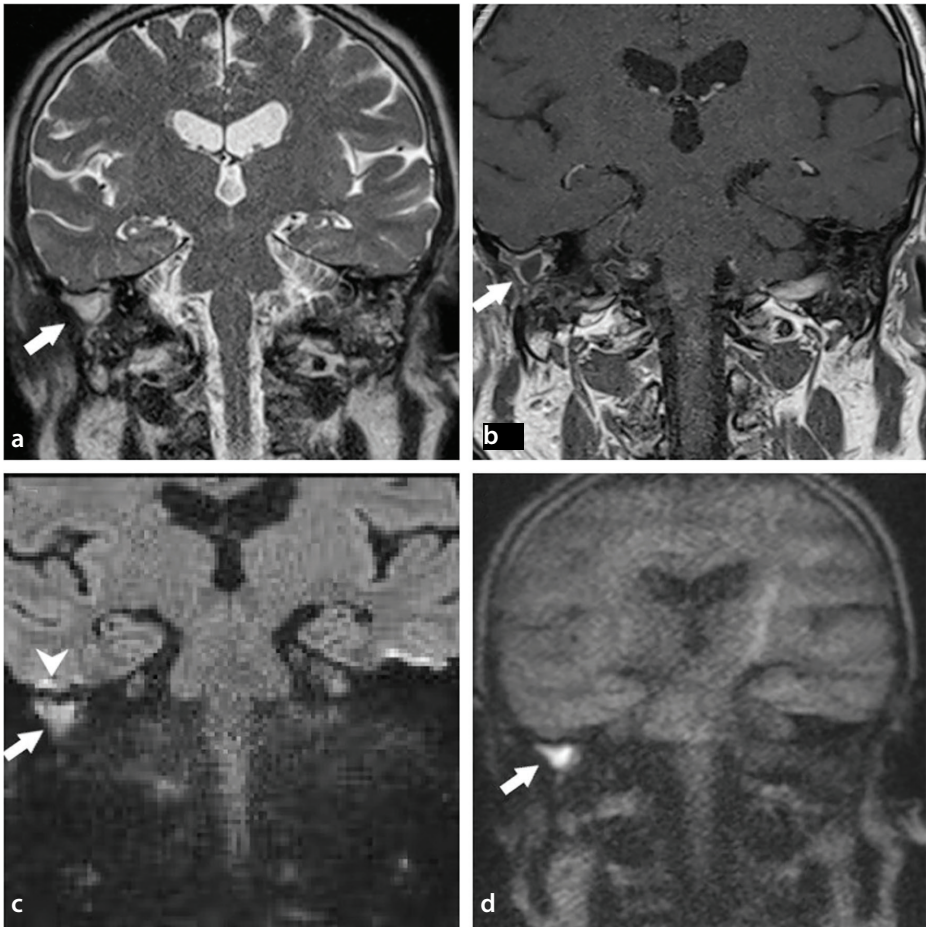

Figure 1. Cholesteatoma case confirmed intraoperatively and histopathologically. A hyperintense lesion (arrow) appears in the middle ear on the coronal T2-weighted image **(a)**, with peripheral contrast enhancement (arrow) visible in the post-contrast T1-weighted coronal image **(b)**. The lesion is also hyperintense (arrow) in readout-segmented (RS)-echo-planar imaging (EPI) **(c)** and non-EPI **(d)** diffusion-weighted images, which is typical for cholesteatoma. Additionally, a susceptibility artifact score of 1 (arrowhead indicating artifact at the skull base) is evident in RS-EPI **(c)**.

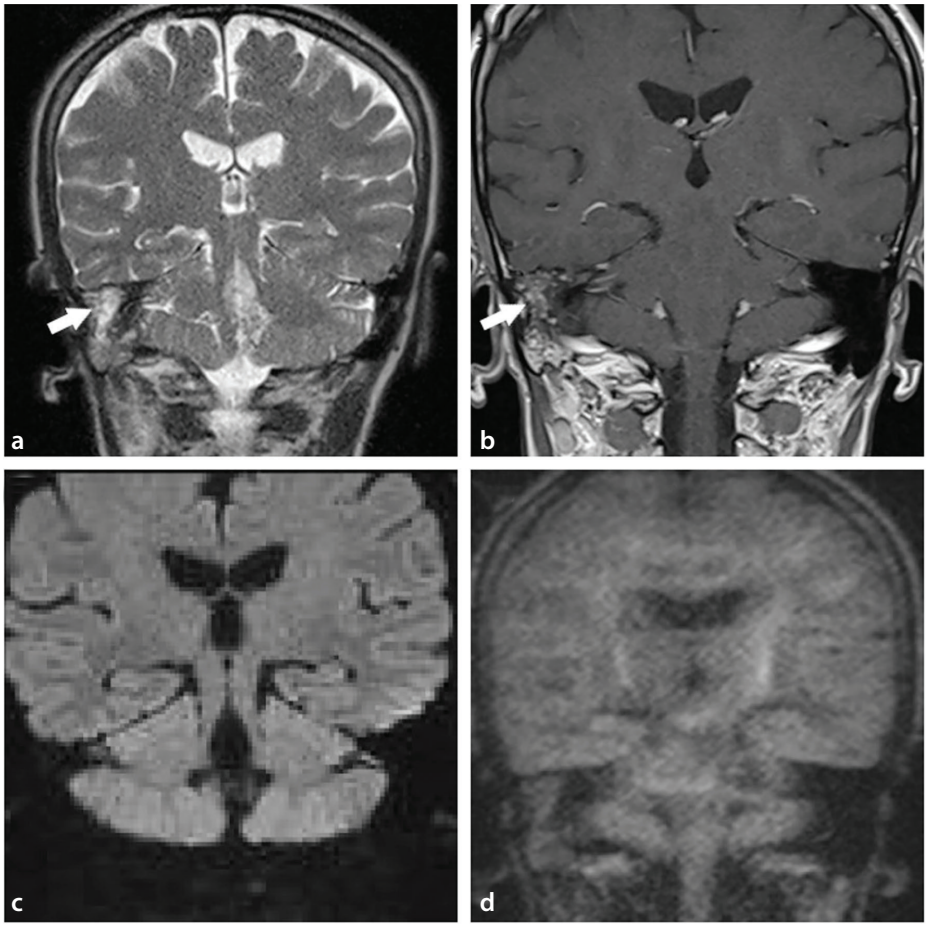

Figure 2. Intraoperatively and histopathologically confirmed case of chronic otitis media (non-cholesteatoma). In the coronal T2-weighted image **(a)**, a hyperintense lesion (arrow) appears in the middle ear. The post-contrast T1-weighted coronal image **(b)** shows homogeneous contrast enhancement (arrow). The lesion, displaying no diffusion restriction in readout-segmented-echo-planar imaging (EPI) **(c)** and non-EPI diffusion-weighted images **(d)**, is consistent with chronic otitis media.

RS-EPI DWI and 50 out of 58 patients (86.2%) using non-EPI DWI. Reader B's specificities in the non-CHO group were 84.5% with RS-EPI DWI (49 out of 58) and 89.7% with non-EPI DWI (52 out of 58).

Table 1 outlines the diagnostic accuracy of CHO detection by Readers A and B across both imaging sequences. Reader A had 10 false negative results in both RS-EPI and non-EPI sequences (10.4% of the CHO group), whereas Reader B recorded false negative results for 17 patients (17.7%) in RS-EPI and for 13 patients (13.5%) in non-EPI.

For false positives in the RS-EPI sequence, Reader A incorrectly diagnosed 12 out of 58 (20.7%) patients with non-CHO and 8 out of 58 (13.8%) in the non-EPI DWI sequence. Reader B identified false positives in 9 out of 58 patients (15.5%) in the RS-EPI DWI sequence and in 6 out of 58 (10.3%) in the non-EPI DWI sequence.

The RS-EPI DWI interobserver agreement coefficient was κ: 0.84 [95% confidence interval (CI): 0.75–0.92], indicating substantial consistency between the readers. Similarly, the non-EPI DWI coefficient was κ: 0.91 (95% CI: 0.84–0.97), signifying a high level of agreement in their interpretations (Table 1).

Reader A measured a minimum CHO size of 2 mm using the RS-EPI DWI sequence and 2.5 mm with the non-EPI DWI sequence. Conversely, Reader B recorded minimum sizes of 2.2 mm for RS-EPI and 1.7 mm for non-EPI DWI sequences. The median values of the longest diameters measured by the readers are detailed in Table 2.

In the group of patients with CHO, Reader A observed the most common contrast enhancement pattern to be peripheral enhancement, occurring at a rate of 66/96 (68.8%); in the non-CHO group, the prevalent pattern was homogeneous enhancement at a rate of 33/58 (56.9%). Reader B reported peripheral enhancement in 73/96 (76.0%) and homogeneous enhancement in 29/58 (50.0%) of cases, respectively. Other contrast enhancement patterns were less frequently observed in both groups (Table 3).

In the analysis of RS-EPI DWI images from 154 patients, the mean ± SD susceptibility artifact score was 1.18 ± 0.70 for Reader A and 1.04 ± 0.41 for Reader B. The mean susceptibility artifact score in non-EPI DWI images was recorded as 0.

Reader A and Reader B measured the SI ratio higher in lesions of the CHO group compared with lesions in the non-CHO group for both RS-EPI and non-EPI DWI sequences. SI measurements were conducted on lesions exhibiting diagnostic hyperintensity. In the non-CHO group, SI measurements consisted of lesions that the readers mistakenly classified as CHO, but histopathological results later confirmed as non-CHO (false positives). Furthermore, both readers noted that the SI ratio in non-EPI DWI images was higher than in RS-EPI DWI images, with measurements of 2.51 for Reader A and 2.46 for Reader B in the CHO group.

The cut-off value for detecting lesions in the CHO and non-CHO groups was determined by averaging the SI measurements of the two readers. In the RS-EPI sequence, the cut-off was >1.15, providing 88.2% specificity, 50% sensitivity, an area under the curve (AUC) of 0.660 (95% CI: 0.547–0.761), and a *P* value of 0.216. For the non-EPI sequence, the cut-off was >1.98, yielding 82.9% sensitivity, 100% specificity, an AUC of 0.901 (95% CI: 0.815–0.956), and a *P* value of <0.001 (Figure 4, Table 4).

The AUC superiority analysis between the RS-EPI and non-EPI sequences showed a difference of 0.241, favoring the non-EPI sequence ($P = 0.042$) (Table 4).

Discussion

In this study, high sensitivity and specificity were achieved with RS-EPI and non-EPI DWI sequences in detecting CHO, with both readers demonstrating consistent results (Table 1). There was a high level of agreement between the readers across both diffusion sequences.

Simultaneous evaluation of RS-EPI DWI and non-EPI DWI images led to enhanced sensitivity in detecting CHO for both readers. Reader A achieved a sensitivity of 91.7%, whereas Reader B reported a sensitivity of 88.5%. The specificity when evaluating RS-EPI alongside non-EPI DWI was comparable to that observed with RS-EPI DWI alone, although it was lower than that observed with non-EPI DWI for both readers (Table 1).

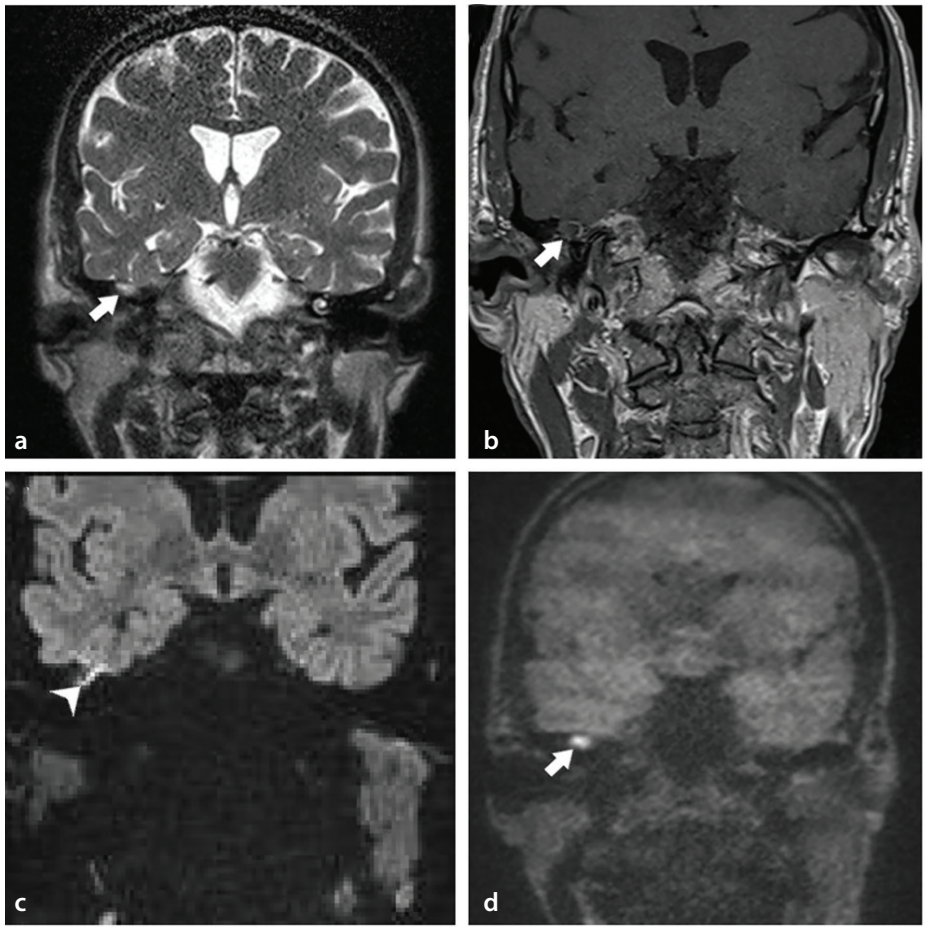

Figure 3. A false positive case in non-echo-planar imaging (EPI) diffusion-weighted imaging (DWI) confirmed histopathologically and intraoperatively as non-cholesteatoma. The lesion in the middle ear is hyperintense (arrow) on the T2-weighted coronal image **(a)** and exhibits peripheral contrast enhancement (arrow) on the post-contrast T1-weighted coronal image (**b**). In readout-segmented-EPI DWI **(c)**, a susceptibility artifact score of 3 (artifact interfering with diagnosis) (arrowhead) is present. Despite appearing hyperintense (arrow) on the non-EPI diffusion-weighted image **(d)**, the lesion has been surgically and histopathologically confirmed to be non-cholesteatoma (false positive).

Wiesmueller et al.'s[9] study, which involved a smaller sample size (n = 25) and used the same device and similar DWI sequence parameters, yielded different results. For TSE DWI, their readers achieved sensitivities of 92% and 88%, respectively, and a specificity of 80% for both. In the case of RESOLVE DWI, the sensitivities were 76% and 68% for readers 1 and 2, respectively, with both readers showing a specificity of 60%. Their study reported an overall agreement of 97% (κ: 0.9) for TSE DWI and 87% (κ: 0.7) for RESOLVE DWI.

In our research, the slice thickness for RESOLVE DWI was 2.5 mm, whereas HASTE DWI had a slice thickness of 3 mm. In contrast, Wiesmueller et al.[9] used a 3-mm slice thickness for both sequences. This difference in slice thickness, in addition to reader-dependent factors, may explain the lower sensitivity and specificity in their RESOLVE DWI compared with ours.

Benson et al.'s[10] study involving 23 participants demonstrated high accuracy in HASTE images, correctly identifying CHO in all patients (100%). In contrast, with RS-EPI sequences, the results were 69.6% positive identifications, 21.7% equivocal, and 8.7% falsely negative. They also observed a substantial degree of interobserver agreement with κ values of 1.0 for HASTE and 0.9 for RS-EPI sequences, highlighting the consistency across readers.

In the present study, the matrix size of the RS-EPI DWI (160 × 104) was smaller than that of the non-EPI DWI (192 × 144). Additionally,

Table 1. Diagnostic performance and interobserver agreement of RS-EPI DWI and non-EPI DWI sequences in diagnosing cholesteatoma

	RS-EPI DWI		Non-EPI DWI		RS-EPI DWI with non-EPI DWI	
	Reader A	Reader B	Reader A	Reader B	Reader A	Reader B
True positive	**86/96** (89.6%)	**79/96** (82.3%)	**86/96** (89.6%)	**83/96** (86.5%)	**88/96** (91.7%)	**85/96** (87.5%)
True negative	**46/58** (79.3%)	**49/58** (84.5%)	**50/58** (86.2%)	**52/58** (89.7%)	**46/58** (79.3%)	**49/58** (84.5%)
False positive	**12/58** (20.7%)	**9/58** (15.5%)	**8/58** (13.8%)	**6/58** (10.3%)	**12/58** (20.7%)	**9/58** (15.5%)
False negative	**10/96** (10.4%)	**17/96** (17.7%)	**10/96** (10.4%)	**13/96** (13.5%)	**8/96** (8.3%)	**11/96** (12.5%)
Sensitivity (%)	**89.6** (81.7–94.9)	**82.3** (73.2–89.3)	**89.6** (81.7–94.9)	**86.5** (78–92.6)	**91.7** (84.2–96.3)	**88.5** (80.4–94.1)
Specificity (%)	**79.3** (66.7–88.8)	**84.5** (72.6–92.7)	**86.2** (74.6–93.7)	**89.7** (78.8–96.1)	**79.3** (66.7–88.8)	**84.5** (72.6–92.7)
LR (+)	**4.3** (2.6–7.2)	**5.30** (2.9–9.7)	**6.5** (3.4–12.4)	**8.36** (3.9–17.9)	**4.4** (2.7–7.4)	**5.7** (3.1–10.5)
LR (-)	**0.1** (0.1–0.2)	**0.21** (0.1–0.3)	**0.1** (0.1–0.2)	**0.15** (0.1–0.3)	**0.1** (0.1–0.2)	**0.1** (0.1–0.2)
Disease pre. (%)	**62.3** (54.2–70)	**62.3** (54.2–70)	**62.3** (54.2–70)	**62.34** (54.2–70)	**62.3** (54.2–70)	**62.3** (54.2–70)
PPV (%)	**87.8** (81.2–92.3)	**89.8** (82.7–94.2)	**91.5** (84.9–95.4)	**93.3** (86.6–96.7)	**88** (81.5–92.4)	**90.4** (83.8–94.5)
NPV (%)	**82.1** (71.6–89.4)	**74.2** (64.9–81.8)	**83.3** (73.4–90.1)	**80** (70.5–87)	**85.2** (74.5–91.9)	**80.7** (71.7–88.7)
Accuracy (%)	**85.7 (79.2–90.8)**	**83.1** (76.3–88.7)	**88.3** (82.2–92.9)	**87.7** (81.4–92.4)	**87** (80.7–91.9)	**87** (80.7–91.9)
Interobserver agreement (κ) (95% CI)	**0.84** (0.75–0.93)		**0.91** (0.84–0.97)		**0.89** (0.81–0.96)	

LR (+), positive likelihood ratio; LR (-), negative likelihood ratio; PPV, positive predictive value; NPV, negative predictive value; κ: Cohen's kappa coefficient; CI, confidence interval; RS-EPI, readout-segmented echo-planar imaging; DWI, diffusion-weighted imaging; non-EPI: non-echo-planar imaging.

Table 2. Quantitative analysis of lesion characteristics in histopathologically confirmed cholesteatoma and non-cholesteatoma groups by Readers A and B

	Reader A					Reader B				
	CHO (Histo)		Non-CHO (Histo)			CHO (Histo)		Non-CHO (Histo)		
	N	Median (IQR)	N	Median (IQR)	*P**	N	Median (IQR)	N	Median (IQR)	*P**
RS-EPI DWI size longest diameter (mm)	86	9.40 (6.30–13.90)	12	9.80 (5.15–11.95)	0.637	79	7.70 (5.00–13.40)	9	6.00 (5.10–9.20)	0.320
RS-EPI DWI SI mean	86	482 (342–571)	12	280 (232–369)	0.003	79	411 (307–503)	9	272 (225–373)	0.026
RS-EPI DWI temporal cortex SI	86	271 (238–298)	12	251 (234–274)	0.293	79	258 (228–281)	9	225 (196–248)	0.097
RS-EPI DWI SI ratio	86	1.66 (1.33–2.33)	12	1.11 (0.91–1.39)	0.003	79	1.56 (1.31–1.88)	9	1.21 (1.09–1.83)	0.116
Non-EPI size longest diameter (mm)	86	10.35 (7.00–14.20)	8	7.15 (5.40–9.45)	0.063	83	8.20 (5.60–12.00)	6	6.60 (5.50–7.70)	0.266
Non-EPI DWI SI mean	86	201 (155–265)	8	134.50 (92.50–161.50)	0.002	83	189 (144–246)	6	157 (114–179)	0.060
Non-EPI DWI temporal. cortex SI	86	81 (74–93)	8	86.5 (77–96)	0.420	83	79 (70–89)	6	89.5 (84–94)	0.185
Non-EPI DWI SI ratio	86	2.51 (1.94–3.06)	8	1.49 (1.19–1.80)	<0.001	83	2.46 (1.92–3.15)	6	1.88 (1.61–2.01)	0.026

*Mann–Whitney test. CHO, cholesteatoma; non-CHO, non-cholesteatoma; RS-EPI, readout-segmented echo-planar imaging; DWI, diffusion-weighted imaging; non-EPI, non-echo-planar imaging; SI, signal intensity; IQR, interquartile range.

Table 3. Comparative lesion characteristics in histopathologically confirmed cholesteatoma and non-cholesteatoma groups by Readers A and B

		Reader A			Reader B		
		Histopathological			Histopathological		
		CHO N (%)	Non-CHO N (%)	*P**	CHO N (%)	Non-CHO N (%)	*P**
T1-weighted signal	Hypointense or isointense	88 (91.7%)	49 (84.5%)	0.266	90 (93.8%)	47 (81.0%)	0.030
	Hyperintense	8 (8.3%)	9 (15.5%)		6 (6.3%)	11 (19.0%)	
Contrast enhancement	No contrast enhancement	2 (2.1%)	0 (0.0%)	NA	15 (15.6%)	3 (5.2%)	<0.001
	Peripheral	66 (68.8%)	12 (20.7%)		73 (76.0%)	15 (25.9%)	
	Homogeneous	14 (14.6%)	33 (56.9%)		7 (7.3%)	29 (50.0%)	
	Heterogeneous	14 (14.6%)	13 (22.4%)		1 (1.0%)	11 (19.0%)	
Location	Middle ear	33 (34.4%)	7 (12.1%)	NA	45 (46.8%)	10 (17.2%)	NA
	Mastoid antrum	3 (3.1%)	1 (1.7%)		2 (2.1%)	4 (6.9%)	
	Both of two	56 (58.3%)	48 (82.8%)		45 (46.9%)	42 (72.4%)	
	Middle ear and EAC	4 (4.2%)	2 (3.4%)		4 (4.2%)	2 (3.4%)	
RS-EPI susceptibility artifact scores	No artifact	14 (14.6%)	4 (6.9%)	NA	3 (3.1%)	6 (10.3%)	NA
	Artifact at the skull base	55 (57.3%)	44 (75.9%)		85 (88.5%)	46 (79.3%)	
	Artifact below the skull base	19 (19.8%)	10 (17.2%)		7 (7.3%)	6 (10.3%)	
	Artifact interfering with diagnosis	8 (8.3%)	0 (0.0%)		1 (1.0%)	0 (0.0%)	
Non-EPI susceptibility artifact scores	No artifact	96 100%)	58 100.%)	NA	96 100%)	58 (100%)	NA

*Chi-square tests. CHO, cholesteatoma; non-CHO, non-cholesteatoma; RS-EPI, readout-segmented echo-planar imaging; non-EPI, non-echoplanar imaging; EAC, external acoustic canal.

the slice thickness for our RS-EPI DWI sequence (2.5 mm) was less than that for the non-EPI DWI (3 mm). Generally, increasing the matrix size improves resolution but may reduce the SNR. Conversely, a thicker slice increases SNR but may compromise resolution.[11] Although the RS-EPI DWI sequence had a smaller matrix size and slice thickness compared with the non-EPI DWI, the resolution was still lower. Despite this, the smaller slice thickness can facilitate better image evaluation.

Fischer et al.'s[12] study, involving 50 patients, found that the sensitivity of RESOLVE DWI in detecting CHO was similar to our results but exhibited higher specificity. They reported an accuracy of 92%, with a sensitivity of 88% and a specificity of 96%.

In light of these findings, non-EPI DWI remains the most effective diffusion sequence for detecting CHO. However, with its shorter imaging times, RS-EPI DWI also proves to be a viable option, boasting high sensitivity and specificity. Reducing the slice thickness, if feasible, may further enhance diagnostic accuracy.

Table 4. Determining signal intensity ratio cut-offs for hyperintense lesions in RS-EPI DWI and non-EPI DWI in cholesteatoma diagnosis

	Signal intensity ratio (reader mean)		
	RS-EPI DWI	Non-EPI DWI	Difference between areas
AUC (95% CI)	0.660 (0.547 to 0.761)	0.901 (0.815 to 0.956)	0.241(0.009–0.474)
p	0.216a	**<0.001**[a]	0.042
$J_{Youden\ index}$	0.382	0.829[a]	-
Cut-off value for cholesteatoma	**>1.15**	**>1.98**	
True positive	67/76 (88.2%)	63/76 82.9%	
True negative	3/6 (50%)	6/6 (100%)	
False positive	3/6 (50%)	0/6 (0.0%)	
False negative	9/76 (11.8%)	13/76 (17.1%)	
Sensitivity (%)	88.2 (78.7–94.4)	82.9 (72.5–90.6)	
Specificity (%)	50 (11.8–88.2)	100 (54.1–100)	
LR (+)	1.8 (0.8– 3.9)	-	
LR (-)	0.2 (0.1–0.7)	0.2 (0.1– 0.3)	
Disease pre. (%)	92.7 (84.8–97.3)	92.68 (84.8–97.3)	
PPV (%)	95.7 (90.9–98.0)	100	
NPV (%)	25 (10.8–47.7)	31.6 (22–43.1)	
Accuracy (%)	85.4 (75.8–92.2)	84.2 (74.4–91.3)	

[a]*p* (area: 0.5). LR (+), positive likelihood ratio; LR (-), negative likelihood ratio; PPV, positive predictive value; NPV, negative predictive value; AUC: area under curve; RS-EPI, readout-segmented echo-planar; DWI, diffusion-weighted imaging; non-EPI, non-echoplanar imaging.

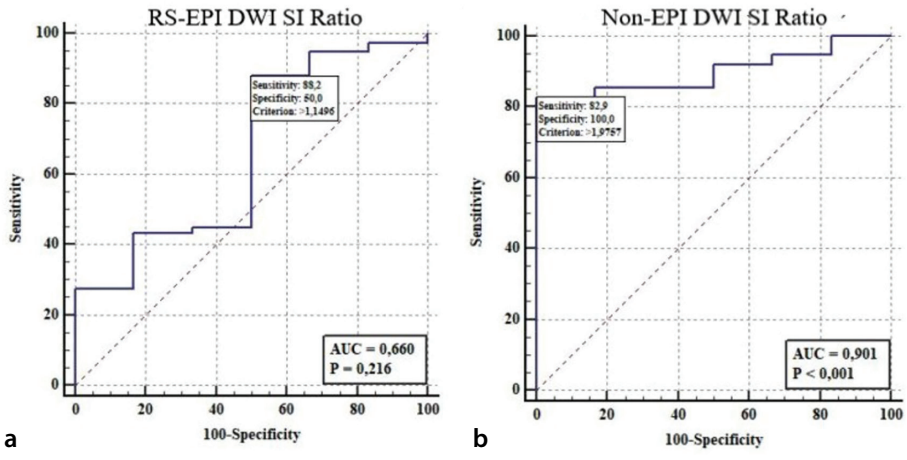

Figure 4. Receiver operating characteristic analysis of signal intensity ratio cut-off in cholesteatoma diagnosis using readout-segmented-echo-planar imaging (EPI) diffusion-weighted imaging (DWI) **(a)** and non-EPI DWI **(b)**.

In the present study, 6 patients exhibited false positives in both RS-EPI and non-EPI DWI images. The histopathological results revealed "granulation tissue with foreign body giant cells" in 1 patient; "polypoid granulation tissue with chronic pyogenic infection" in another; "inflammatory pseudopolyp and granulation tissue" in 2 patients; and "chronic inflammatory granulation tissue" in 2 other patients. Additionally, other cases of false positives in either RS-EPI or non-EPI DWI images were diagnosed with "chronic inflammatory granulation tissue."

The literature identifies several entities as potential sources of false positives, including cholesterol granuloma,[13] earwax,[14] abscesses,[15] ceruminous adenomas,[16] and bone grafts.[17]

The literature reveals varying rates of false positives in CHO detection using DWI MRI. A study by Muhonen et al.[18] showed that out of 27 patients who underwent second-look surgery after detecting increased SI on non-EPI DWI, two cases (7.4%) were identified as false positives. Another study by Semiz-Oysu et al.[19], which involved 112 ears, reported five cases (4.5%) as false positives.

Reducing the false positive rate could minimize unnecessary surgical interventions and reduce the frequency of second-look surgeries. In the present study, we conducted SI measurements on two DWI sequences to differentiate between false positives and true positive cases, establishing a cut-off value in non-EPI DWI. The literature on this subject is sparse. Özgen et al.[20] established an SI ratio cut-off of 0.9 in TSE-DWI images, achieving 100% sensitivity and specificity in distinguishing between CHO and non-CHO in 57 patients. In contrast, our investigation focused solely on lesions identified with hyperintensity on DWI, and we established a cut-off value to discern the more challenging cases of true positives and false positives. Consequently, a substantially higher cut-off value was identified in our study.

Specifically, in the present study, when the SI ratio in the non-EPI DWI sequence exceeded the established cut-off value of 1.98, the consideration of CHO was supported by high sensitivity and specificity. The reported values are as follows: sensitivity 82.9% and specificity 100%. The RS-EPI DWI sequence demonstrated a cut-off value with lower sensitivity and specificity, reporting a sensitivity of 88.2% and a specificity of 50% (Table 4). To the best of our knowledge, no existing study has measured SI in both diffusion sequences and established cut-off values. Further research in this area is warranted, and our findings could pave the way for future investigations.

Dudau et al.[21] reported an average artifact score of 0.73 for RS-EPI (range: 0–3), assessing all 426 scored entries. They also found an average artifact score of 0 for non-EPI DWI, aligning with our results. The increased susceptibility artifact in RS-EPI DWI, compared with non-EPI DWI, may contribute to a higher incidence of false-negative results in RS-EPI DWI for Reader B. By implementing measures to reduce susceptibility artifacts, we can enhance both the utilization and diagnostic performance of the RS-EPI DWI technique.

It is widely acknowledged that non-EPI techniques exhibit fewer susceptibility artifacts at the skull base compared with EPI techniques.[22] However, in the present study, when examining the artifact score distribu-

tion in RS-EPI DWI, Reader A reported "artifact interfering with diagnosis" in 8 images (5.2%), whereas Reader B reported it in only 1 image (0.65%) (Table 3). This suggests that while RS-EPI DWI may present more artifacts compared with non-EPI DWI, these do not substantially affect the diagnosis.

This study has certain limitations. First, it was conducted retrospectively, which may have influenced the outcomes. Additionally, there were differences in slice thickness between RS-EPI DWI and non-EPI DWI. The measurement of SI was performed manually using a ROI. Despite efforts to minimize bias through the involvement of two readers and averaging their measurements for the cut-off assessment, acknowledging the potential limitations due to individual practitioner variability remains important.

To validate and expand upon the findings of this research, conducting prospective studies with a larger sample size is recommended. Increasing the number of studies that thoroughly evaluate SI measurements will contribute to a more nuanced understanding of DWI in the diagnosis of CHO. Future research should prioritize efforts to mitigate susceptibility artifacts in RS-EPI DWI acquisition while maintaining an optimal acquisition time.

In conclusion, our research suggests that both non-EPI and RS-EPI DWI sequences effectively detect CHO with notable sensitivity and specificity when used individually. While RS-EPI DWI does not serve as a substitute for non-EPI DWI, integrating both sequences may enhance overall sensitivity. The assessment of SI in DWI appears to be beneficial for diagnosing CHO. Moreover, establishing an SI ratio cut-off value seems to reliably differentiate between CHO and non-CHO with high precision. Finally, RS-EPI DWI demonstrated minimal susceptibility artifacts, which did not substantially affect the diagnostic accuracy.

Conflict of interest disclosure

The authors declared no conflicts of interest.

References

1. Schürmann M, Goon P, Sudhoff H. Review of potential medical treatments for middle ear cholesteatoma. *Cell Commun Signal*. 2022;20(1):148. [CrossRef]
2. Henninger B, Kremser C. Diffusion weighted imaging for the detection and evaluation of cholesteatoma. *World J Radiol*. 2017;9(5):217-222. [CrossRef]
3. Bammer R. Basic principles of diffusion-weighted imaging. *Eur J Radiol*. 2003;45(3):169-184. [CrossRef]
4. Vercruysse JP, De Foer B, Pouillon M, Somers T, Casselman J, Offeciers E. The value of diffusion-weighted MR imaging in the diagnosis of primary acquired and residual cholesteatoma: a surgical verified study of 100 patients. *Eur Radiol*. 2006;16(7):1461-1467. [CrossRef]
5. Fischer N, Plaikner M, Schartinger VH, et al. MRI of middle ear cholesteatoma: the importance of observer reliance from diffusion sequences. *J Neuroimaging*. 2022;32(1):120-126. [CrossRef]
6. Schwartz KM, Lane JI, Bolster BD Jr, Neff BA. The utility of diffusion-weighted imaging for cholesteatoma evaluation. *AJNR Am J Neuroradiol*. 2011;32(3):430-436. [CrossRef]
7. Muzaffar J, Metcalfe C, Colley S, Coulson C. Diffusion-weighted magnetic resonance imaging for residual and recurrent cholesteatoma: a systematic review and meta-analysis. *Clin Otolaryngol*. 2017;42(3):536-543. [CrossRef]
8. Moustin D, Veillon F, Karch-Georges A, et al. Importance of signal intensity on T1-weighted spin-echo sequence for the diagnosis of chronic cholesteatomatous otitis. *Eur Arch Otorhinolaryngol*. 2020;277(6):1601-1608. [CrossRef]
9. Wiesmueller M, Wuest W, May MS, et al. Comparison of readout-segmented echo-planar imaging and single-shot TSE DWI for cholesteatoma diagnostics. *AJNR Am J Neuroradiol*. 2021;42(7):1305-1312. [CrossRef]
10. Benson JC, Carlson ML, Lane JI. Non-EPI versus multishot EPI DWI in cholesteatoma detection: Correlation with operative findings. *Am J Neuroradiol*. 2021;42(3):573-577. [CrossRef]
11. McRobbie DW, Moore EA, Graves MJ, Prince MR. MRI from picture to proton. *MRI from Pict to Prot*. Published online January 1, 2006:1-397. [CrossRef]
12. Fischer N, Schartinger VH, Dejaco D, et al. Readout-segmented echo-planar DWI for the detection of cholesteatomas: correlation with surgical validation. *AJNR Am J Neuroradiol*. 2019;40(6):1055. [CrossRef]
13. Fukuda A, Morita S, Harada T, et al. Value of T1-weighted magnetic resonance imaging in cholesteatoma detection. *Otol Neurotol*. 2017;38(10):1440-1444. [CrossRef]
14. Zaman SU, Rangankar VP, Krishnarjun M, et al. Readout-segmented echoplanar (RESOLVE) diffusion-weighted imaging on 3T MRI in detection of cholesteatoma-our experience. *Indian J Radiol Imaging*. 2023;34(1)16-24. [CrossRef]
15. Profant M, Sláviková K, Kabátová Z, Slezák P, Waczulíková I. Predictive validity of MRI in detecting and following cholesteatoma. *Eur Arch Oto-Rhino-Laryngology*. 2012;269(3):757-765. [CrossRef]
16. Esmaili AA, Hasan Z, Withers SJ, Kuthubutheen J. A retrospective cohort study on false positive diffusion weighted MRI in the detection of cholesteatoma. *Aust J Otolaryngol*. 2021;4:18. [CrossRef]
17. Osman NM, Rahman AA, Ali MT. The accuracy and sensitivity of diffusion-weighted magnetic resonance imaging with apparent diffusion coefficients in diagnosis of recurrent cholesteatoma. *Eur J Radiol Open*. 2017;4:27. [CrossRef]
18. Muhonen EG, Mahboubi H, Moshtaghi O, et al. False-Positive cholesteatomas on non-echoplanar diffusion-weighted magnetic resonance imaging. *Otol Neurotol*. 2020;41(5):588-592. [CrossRef]
19. Semiz-Oysu A, Oysu C, Kulali F, Bukte Y. PROPELLER diffusion weighted imaging for diagnosis of cholesteatoma in comparison with surgical and histopathological results: emphasis on false positivity and false negativity. *Eur Arch Otorhinolaryngol*.2023;280(11):4845-4850. [CrossRef]
20. Özgen B, Bulut E, Dolgun A, Bajin MD, Sennaroğlu L. Accuracy of turbo spin-echo diffusion-weighted imaging signal intensity measurements for the diagnosis of cholesteatoma. *Diagn Interv Radiol*. 2017;23(4):300-306. [CrossRef]
21. Dudau C, Draper A, Gkagkanasiou M, Charles-Edwards G, Pai I, Connor S. Cholesteatoma: multishot echo-planar vs non echo-planar diffusion-weighted MRI for the prediction of middle ear and mastoid cholesteatoma. *BJR|Open*. 2019;1(1):20180015. [CrossRef]
22. De Foer B, Vercruysse JP, Bernaerts A, et al. Detection of postoperative residual cholesteatoma with non-echo-planar diffusion-weighted magnetic resonance imaging. *Otol Neurotol*. 2008;29(4):513-517. [CrossRef]